v7.n12.2026

SCIENTIFIC JOURNAL - RECIMA21 ISSN 2675-6218

DROUGHT VARIABILITY IN AFRÂNIO, PERNAMBUCO: ANALYSIS OF SPI SERIES AT MULTIPLE TIMESCALES VIA COMPLEXITY-ENTROPY CAUSALITY PLANE (CECP)

VARIABILIDADE DAS SECAS EM AFRÂNIO, PERNAMBUCO: ANÁLISE DE SÉRIES SPI EM MÚLTIPLAS ESCALAS TEMPORAIS PELO PLANO DE CAUSALIDADE DE COMPLEXIDADE-ENTROPIA (CECP)

VARIABILIDAD DE LAS SEQUÍAS EN AFRÂNIO, PERNAMBUCO: ANÁLISIS DE SERIES SPI EN MÚLTIPLES ESCALAS TEMPORALES MEDIANTE EL PLANO DE CAUSALIDAD DE COMPLEJIDAD-ENTROPÍA (CECP)

Antônio Victor Alves Silva[1], Antonio Samuel Alves da Silva[2], Tatijana Stosic[3]

https://doi.org/10.47820/recima21.v7i12.9653

PUBLISHED: 12/2026

ABSTRACT

This study analyzed drought variability in Afrânio, Pernambuco, using the Standardized Precipitation Index (SPI) and the Complexity-Entropy Causality Plane (CECP). Monthly rainfall records (1950–2012; 756 observations) were converted into SPI series at 1-, 3-, 6-, and 12-month timescales using the Gamma distribution. The CECP was applied to the full record and to two 30-year subperiods (1953–1982 and 1983–2012). Extreme droughts (SPI ≤ −2) occurred at the 3-, 6-, and 12-month scales, with 1976 as the most severe year (SPI-6 = −4.00). SPI-1 was close to white noise (entropy = 0.954; complexity = 0.075), whereas longer timescales showed lower entropy and higher complexity, indicating greater temporal organization (SPI-12: 0.852 and 0.206), partly associated with SPI accumulation. Differences between subperiods were small and descriptive. Overall, the CECP complemented the SPI by describing how drought-related variability is organized across accumulation timescales in Afrânio.

KEYWORDS: *Standardized Precipitation Index (SPI). Complexity-Entropy Causality Plane (CECP). Drought. Afrânio-PE.*

RESUMO

Este estudo analisou a variabilidade das secas em Afrânio, Pernambuco, utilizando o Índice de Precipitação Padronizada (SPI) e o Plano de Causalidade de Complexidade-Entropia (CECP). Registros mensais de chuva (1950–2012; 756 observações) foram convertidos em séries SPI nas escalas de 1, 3, 6 e 12 meses, por meio da distribuição Gama. O CECP foi aplicado à série completa e a dois subperíodos de 30 anos (1953–1982 e 1983–2012). Secas extremas (SPI ≤ −2) ocorreram nas escalas de 3, 6 e 12 meses, com 1976 como o ano mais severo (SPI-6 = −4,00). O SPI-1 ficou próximo ao ruído branco (entropia = 0,954; complexidade = 0,075), enquanto escalas maiores apresentaram menor entropia e maior complexidade, indicando maior organização temporal (SPI-12: 0,852 e 0,206), em parte associada à acumulação do SPI. As diferenças entre os subperíodos foram pequenas e descritivas.

[1]Federal Rural University of Pernambuco (UFRPE). Bachelor in Statistics (UEPB) and M.Sc. student in Biometrics and Applied Statistics at UFRPE, working in time series analysis and applied statistics.
[2]Federal Rural University of Pernambuco (UFRPE). Ph.D. in Biometrics and Applied Statistics (UFRPE) and professor at UFRPE, working in applied statistics and environmental data analysis.
[3]Federal Rural University of Pernambuco (UFRPE). Ph.D. in Statistical Physics (University of Belgrade) and professor at UFRPE, working in statistical physics applied to environmental and hydrological data.

This article is published in open access under the Creative Commons Attribution 4.0 International (CC BY 4.0) license, which permits unrestricted use, distribution, and reproduction in any medium, provided that the original author and source are credited.

De modo geral, o CECP complementou o SPI ao descrever como a variabilidade ligada às secas se organiza nas diferentes escalas de acumulação em Afrânio.

PALAVRAS-CHAVE: Índice de Precipitação Padronizada (SPI). Plano de Causalidade de Complexidade-Entropia (CECP). Seca. Afrânio-PE.

RESUMEN
Este estudio analizó la variabilidad de las sequías en Afrânio, Pernambuco, utilizando el Índice de Precipitación Estandarizada (SPI) y el Plano de Causalidad de Complejidad-Entropía (CECP). Registros mensuales de lluvia (1950–2012; 756 observaciones) fueron convertidos en series SPI en las escalas de 1, 3, 6 y 12 meses, mediante la distribución Gamma. El CECP se aplicó a la serie completa y a dos subperíodos de 30 años (1953–1982 y 1983–2012). Ocurrieron sequías extremas (SPI ≤ −2) en las escalas de 3, 6 y 12 meses, con 1976 como el año más severo (SPI-6 = −4,00). El SPI-1 se mantuvo cercano al ruido blanco (entropía = 0,954; complejidad = 0,075), mientras que las escalas mayores presentaron menor entropía y mayor complejidad, indicando mayor organización temporal (SPI-12: 0,852 y 0,206), en parte asociada a la acumulación del SPI. Las diferencias entre los subperíodos fueron pequeñas y descriptivas. En general, el CECP complementó el SPI al describir cómo se organiza la variabilidad asociada a las sequías en las distintas escalas de acumulación en Afrânio.

PALABRAS CLAVE: *Índice de Precipitación Estandarizada (SPI). Plano de Causalidad de Complejidad-Entropía (CECP). Sequía. Afrânio-PE.*

1. INTRODUCTION

Extreme drought events occur when precipitation remains below normal levels for extended periods. They affect ecosystems, human populations, agriculture, transportation, and water supply systems (Silva *et al.*, 2025). This situation is characteristic of the municipality of Afrânio, located in the semi-arid region of northeastern Brazil, within the São Francisco mesoregion and the Petrolina microregion. The municipality borders the state of Piauí to the north and west, Bahia to the south, and the municipalities of Dormentes and Petrolina to the east (Beltrão *et al.*, 2005). Covering an area of 1,482.4 km², equivalent to approximately 1.5% of the state of Pernambuco, and situated within the Brazilian Drought Polygon (Santiago *et al.*, 2019), Afrânio experiences highly irregular rainfall patterns in both time and space. These climatic conditions have historically constrained socioeconomic development and compromised local livelihoods.

To characterize and monitor drought events, several standardized indices have been developed, including the Standardized Precipitation Index (SPI) (McKee *et al.*, 1993), the Palmer Drought Severity Index (PDSI) (Palmer, 1965), and the Standardized Precipitation Evapotranspiration Index (SPEI) (Vicente-Serrano *et al.*, 2010). Among these, the SPI has become one of the most widely used indicators for meteorological drought assessment due to its

This article is published in open access under the Creative Commons Attribution 4.0 International (CC BY 4.0) license, which permits unrestricted use, distribution, and reproduction in any medium, provided that the original author and source are credited.

simplicity, flexibility across multiple timescales, and reliance solely on precipitation data. Following the recommendations of the Lincoln Declaration on Drought Indices, National Meteorological and Hydrological Services (NMHSs) have been encouraged to adopt the SPI as the standard tool for characterizing meteorological droughts, a recommendation subsequently endorsed and promoted by the World Meteorological Organization (WMO) (Hayes *et al.*, 2011). However, while the SPI effectively quantifies drought severity, duration, and frequency, traditional index-based analyses alone do not capture underlying shifts in the temporal organization, predictability, or nonlinear dynamics of hydroclimatic regimes.

As a complement to the SPI, this study employed the Complexity-Entropy Causality Plane (CECP), a methodology founded on the permutation entropy framework proposed by Bandt and Pompe (2002). The CECP provides a graphical representation that positions different dynamical regimes within distinct regions of the entropy-complexity space. It discriminates between Gaussian and non-Gaussian processes and identifies varying degrees of temporal correlation. These properties make the method particularly suitable for real-world data, which are inherently affected by noise and complex dynamics, and offer an objective framework for characterizing and comparing time-series behavior. As emphasized by Rosso *et al.* (2007), the CECP is effective in distinguishing stochastic noise from deterministic chaos, which supports its application alongside climatological indices.

The use of this methodology provides a basis for investigating the balance between order and disorder in drought regimes and for assessing the temporal organization underlying hydroclimatic variability. Its application is supported by the robustness of the CECP when dealing with relatively short and noisy time series (Rosso *et al.*, 2012), as well as by its increasing use in the analysis of Brazilian environmental systems. For example, studies of rainfall variability in the Brazilian semi-arid region have shown that El Niño events reduce statistical complexity, which reflects a shift toward more deterministic climatic dynamics (Silva *et al.*, 2021a). Specifically in Afrânio, recent research using the Rainfall Anomaly Index (RAI) identified a succession of dry years between 1994 and 2023 linked to the warm phase of the El Niño-Southern Oscillation (ENSO) (Vieira & Lira, 2025). This reflects the broader recurrence and spatiotemporal variability of meteorological droughts documented across the Brazilian semi-arid region (Brito *et al.*, 2021). Nevertheless, because conventional anomaly indices focus primarily on rainfall magnitude, it remains unclear whether these drought episodes also alter the intrinsic complexity and temporal structure of drought regimes at the local scale.

Although SPI is widely used for drought monitoring, to the authors' knowledge, the combined use of the SPI and the CECP to investigate drought dynamics has not yet been

This article is published in open access under the Creative Commons Attribution 4.0 International (CC BY 4.0) license, which permits unrestricted use, distribution, and reproduction in any medium, provided that the original author and source are credited.

explored in Afrânio-PE. Understanding the temporal behavior of SPI series across different accumulation timescales can improve the interpretation and application of this index in water resources monitoring and management, particularly in semi-arid regions. This study addresses the following question: how does the joint application of the SPI and the CECP characterize the temporal variability of droughts in Afrânio, Pernambuco, considering different accumulation timescales and historical periods? Therefore, the main objective of this study was to evaluate the temporal dynamics of the drought regime in Afrânio, Pernambuco, using both the SPI and the CECP framework. Specifically, the study aimed to: (i) calculate the SPI at 1-, 3-, 6-, and 12-month timescales and identify years characterized by extreme drought conditions (SPI ≤ −2); (ii) characterize the dynamics of each SPI series through CECP metrics of entropy and statistical complexity; (iii) compare the temporal behavior of two 30-year subperiods (1953–1982 and 1983–2012); and (iv) assess how the entropy-complexity structure evolves with increasing SPI timescale.

To do this, monthly rainfall records (1950–2012) from the LAMEP/ITEP station in Afrânio were converted into SPI series at 1-, 3-, 6-, and 12-month timescales. Each series was then analyzed with the CECP, using normalized permutation entropy and statistical complexity, for the full record and for two 30-year subperiods.

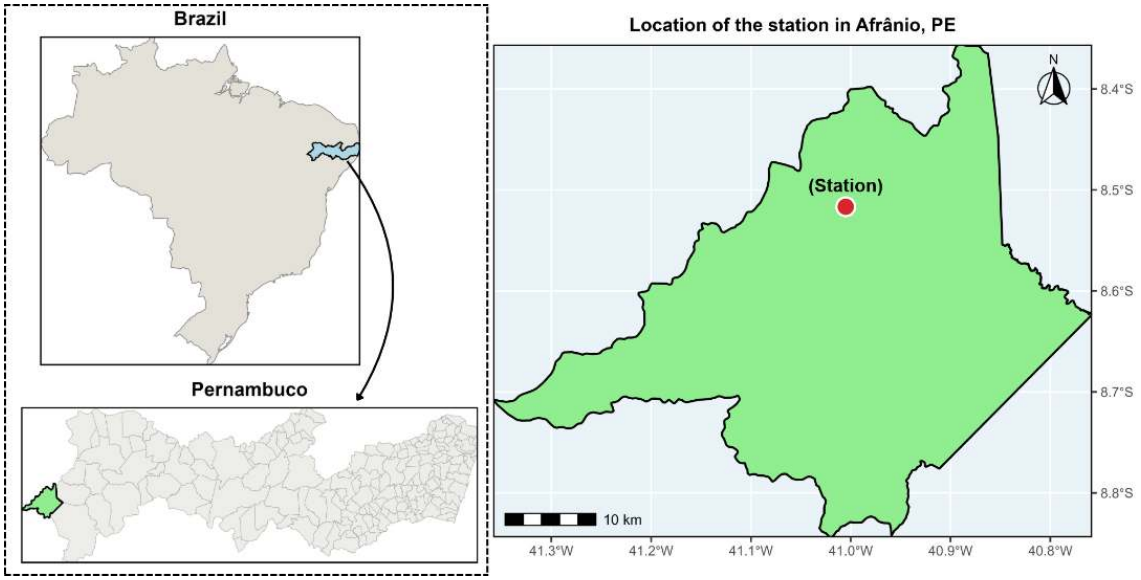
2. METHODOLOGY

2.1. Study area and dataset

For the analysis of drought history, monthly precipitation data from the meteorological station located in Afrânio, Pernambuco (8°31′00″ S, 41°00′18″ W), were used. The dataset spans the period from January 1950 to December 2012, comprising 756 monthly observations and covering a total of 63 years. The precipitation records were obtained from the Meteorological Laboratory of the Institute of Technology of Pernambuco (*Laboratório de Meteorologia do Instituto de Tecnologia de Pernambuco, LAMEP/ITEP*), the same series previously described by Santiago *et al.* (2019). The location of the meteorological station in the municipality of Afrânio (PE) is shown in Figure 1.

This article is published in open access under the Creative Commons Attribution 4.0 International (CC BY 4.0) license, which permits unrestricted use, distribution, and reproduction in any medium, provided that the original author and source are credited.

Figure 1. Geographic location of the Afrânio meteorological station in the state of Pernambuco, northeastern Brazil.



Source: Authors

2.2. Standardized precipitation index (SPI)

The Standardized Precipitation Index (SPI) was originally proposed by McKee *et al.* (1993) and later further developed by Edwards and McKee (1997). It is one of the most widely used indices for the quantitative characterization and monitoring of droughts across multiple timescales. For a given timescale, a drought event is defined as a period during which the SPI remains continuously negative and reaches a value of −1.0 or lower in at least one month. The onset of a drought is identified when the SPI first becomes negative, whereas its termination occurs when the index returns to positive values following a period in which it has reached or fallen below −1.0. According to the classification proposed by McKee *et al.* (1993), both dry and wet conditions can be categorized into different intensity classes based on SPI values, as follows:

This article is published in open access under the Creative Commons Attribution 4.0 International (CC BY 4.0) license, which permits unrestricted use, distribution, and reproduction in any medium, provided that the original author and source are credited.

Table 1. Dry/wet categories of the Standardized Precipitation Index (SPI). Source: Svoboda *et al.* (2012)

SPI classification	SPI value
Extremely dry	SPI ≤ −2
Severely dry	−2 < SPI ≤ −1.5
Moderately dry	−1.5 < SPI ≤ −1.0
Near Normal	−1.0 < SPI < 1.0
Moderately wet	1.0 ≤ SPI < 1.5
Very wet	1.5 ≤ SPI < 2.0
Extremely wet	SPI ≥ 2.0

In this study, the 1-, 3-, 6- and 12-month SPI are used to represent short, intermediate, and long-term dry/wet conditions.

The calculation of the SPI consists of fitting the historical series of accumulated precipitation, for a given time scale, to a two-parameter Gamma probability distribution, whose shape (α) and scale (β) parameters are estimated by the maximum likelihood method (Thom, 1966). Subsequently, the cumulative probability distribution is transformed into a standard normal distribution (zero mean and unit standard deviation), so that the SPI represents the number of standard deviations by which the observed precipitation deviates from the historical mean for the period and location considered.

The Gamma distribution is defined by its probability density function (Eq. 1):

$$g(x) = \frac{1}{\beta^{\alpha}\Gamma(\alpha)} x^{\alpha-1} e^{-x/\beta}, \quad x > 0 \tag{1}$$

where $\alpha > 0$ is the shape parameter, $\beta > 0$ is the scale parameter, x is the amount of precipitation, and $\Gamma(\alpha)$ is the gamma function, defined by the integral (Wilks, 2011) (Eq. 2):

$$\Gamma(\alpha) = \int_0^{\infty} t^{\alpha-1} e^{-t}\, dt \tag{2}$$

The parameters α and β are estimated for each month and for each time scale of interest using the maximum likelihood method proposed by Thom (1966) (Eq. 3 and Eq. 4):

$$\hat{\alpha} = \frac{1}{4A}\left(1 + \sqrt{1 + \frac{4A}{3}}\right), \qquad \hat{\beta} = \frac{\bar{x}}{\hat{\alpha}} \tag{3}$$

where

$$A = \ln(\bar{x}) - \frac{\sum \ln(x)}{n} \tag{4}$$

in which n is the number of precipitation observations.

2.3. Complexity-entropy causality plane (CECP)

The characterization of the temporal dynamics of SPI was conducted using the Complexity-Entropy Causality Plane (CECP), a theoretical framework established by Rosso et al. (2007) for discriminating deterministic, stochastic, and periodic time series. Fundamentally, the

This article is published in open access under the Creative Commons Attribution 4.0 International (CC BY 4.0) license, which permits unrestricted use, distribution, and reproduction in any medium, provided that the original author and source are credited.

plane is constructed from two complementary metrics: the normalized permutation entropy (H_s) and the permutation statistical complexity (C), whose values depend exclusively on the probability distribution of ordinal patterns extracted from the series under analysis, as in the procedure of Bandt and Pompe (2002).

The implementation of the method requires the choice of embedding parameters. For a series $\{x_t\}_{t=1,\ldots,N}$, a sliding window of length d (embedding dimension) and time delay τ is defined. To each vector $(x_t, x_{t+\tau}, \ldots, x_{t+(d-1)\tau})$, an ordinal pattern π is associated, representing the relative order (*rank*) of its elements. The relative frequency $p(\pi)$ of each of the $d!$ possible patterns along the entire series is then counted. The reliability of these estimates, however, is subject to a fundamental condition: the length of the series must be substantially greater than the number of possible ordinal patterns ($d!$), usually $N \geq 5d!$ (Bandt & Pompe, 2002; Riedl *et al.*, 2013). In this study, *d* = 5 and $\tau = 1$ were adopted, since the dataset under consideration satisfies this minimum length requirement. With *d* = 5, the state space accommodates 120 possible ordinal patterns.

To assess potential changes in drought dynamics associated with climate variability and change, the analyzed series were divided into two 30-year subperiods (1953–1982 and 1983–2012), as in the climatological standard recommended by the World Meteorological Organization (WMO). The first three years of the record (1950–1952) were excluded from this subperiod analysis so that both periods had equal length (30 years each) for a symmetric comparison. The CECP analysis was then repeated for each subperiod to enable a comparative evaluation of their temporal dynamics. To ensure statistical robustness in the estimation of ordinal pattern probability distributions, the embedding dimension was reduced from 5 to 4, which yields 24 possible ordinal patterns. This adjustment is appropriate for shorter time series and helps maintain the reliability of the entropy and complexity estimates.

Once the empirical probabilities are obtained, the permutation entropy $H(d)$ is calculated in the classical Shannon entropy formulation (Eq. 5):

$$H(d) = -\sum_{\pi} p(\pi)\log_2 p(\pi), \quad (5)$$

Its values range from 0, corresponding to a perfectly ordered series (strictly increasing or decreasing) to $\log_2(\mathrm{d}!)$, which characterizes a completely random process in which all ordinal patterns are equally probable. To facilitate comparisons among different configurations, the normalized permutation entropy H_s is defined as $H_s = H/\log_2(d!)$, such that $0 \leq H_s[P] \leq 1$.

However, entropy alone is insufficient to characterize the underlying structure of a dynamical system, since different systems may exhibit the same degree of disorder while possessing markedly different levels of organization. To overcome this limitation, Rosso *et al.*

This article is published in open access under the Creative Commons Attribution 4.0 International (CC BY 4.0) license, which permits unrestricted use, distribution, and reproduction in any medium, provided that the original author and source are credited.

(2007) proposed the Jensen-Shannon statistical complexity, defined as the product of normalized entropy and the normalized Jensen-Shannon divergence with respect to the uniform distribution:

$$C[P] = \frac{J[P,P_e]}{J_{max}} \cdot H_s[P], \qquad 0 \leq C[P] \leq 1. \tag{6}$$

The quantity $J[P,P_e]$ represents the Jensen-Shannon divergence,

$$J[P,P_e] = S\left[\frac{P+P_e}{2}\right] - \frac{1}{2}S[P] - \frac{1}{2}S[P_e], \tag{7}$$

where $S[\mathrm{P}]$ denotes the Shannon entropy (in bits) associated with the probability distribution P, and J_{max} is a normalization constant corresponding to the maximum possible divergence, when all probability mass is concentrated in a single ordinal pattern while the remaining probabilities are zero (Lamberti *et al.*, 2004). The value of J_{max} is therefore expressed as (Eq. 8):

$$J_{max} = -\frac{1}{2}\left[\frac{d!+1}{d!}\log(d!+1) - 2\log(2d!) + \log(d!)\right]. \tag{8}$$

Consequently, $C[P] = 0$ for a completely random process ($H_s = 1, J = 0$) and for regular periodic processes ($H_s = 0$). Intermediate and relatively high complexity values emerge when the system exhibits non-trivial temporal correlations and structured dynamics, which indicate the coexistence of order and randomness. Such regimes are often associated with complex natural processes that cannot be adequately described as either purely stochastic or fully deterministic.

By representing the entropy-complexity pair (H_s, C) in the two-dimensional space, the CECP provides both a visual and quantitative framework for diagnosing the underlying dynamics of a time series. As demonstrated by Rosso *et al.* (2007), periodic and quasi-periodic processes tend to cluster in the lower-left region of the plane, characterized by low entropy and low complexity. In contrast, uncorrelated stochastic processes, such as white noise, are typically located in the lower-right region, where entropy is high and complexity remains low. Systems exhibiting deterministic chaos, non-linear behavior, or long-range temporal correlations occupy the upper regions of the plane, where statistical complexity reaches its highest values for a given level of entropy.

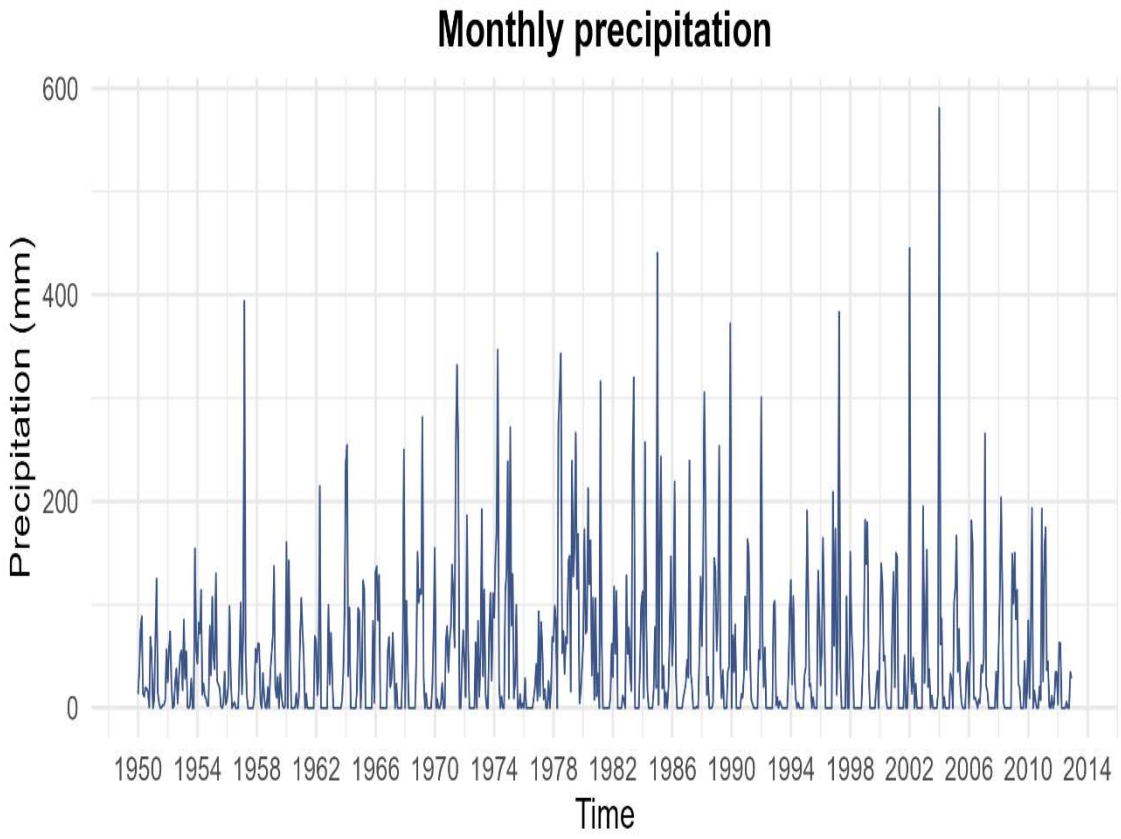
Furthermore, the CECP is bounded by theoretical curves of minimum and maximum complexity, analytically derived for the selected embedding dimension. These boundaries define the admissible region of the entropy-complexity space and provide an invariant reference framework for the interpretation and comparison of different dynamical systems (Rosso *et al.*, 2007). Consequently, the CECP enables the identification and classification of distinct dynamical regimes. It offers valuable insights into the degree of randomness, organization, and temporal structure present in the analyzed series.

This article is published in open access under the Creative Commons Attribution 4.0 International (CC BY 4.0) license, which permits unrestricted use, distribution, and reproduction in any medium, provided that the original author and source are credited.

3. RESULTS AND DISCUSSION

Using the monthly precipitation series for the period 1950–2012 (Figure 2), SPI series were calculated at the 1-, 3-, 6-, and 12-month timescales according to the methodology of McKee *et al.* (1993) and Svoboda *et al.* (2012). The resulting SPI series are presented in Figure 3.

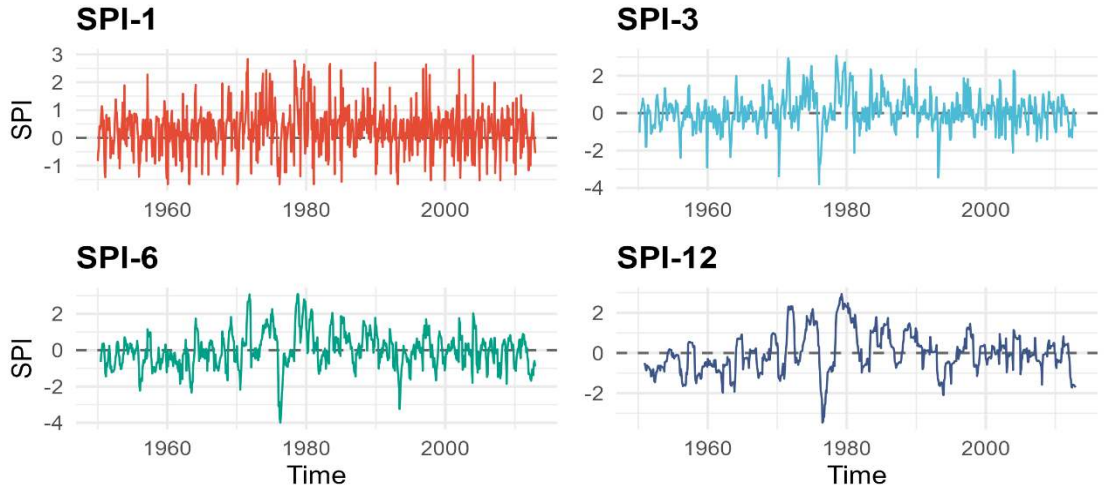
Figure 2. Monthly precipitation series recorded at the Afrânio meteorological station during the period from January 1950 to December 2012.



Source: Authors

This article is published in open access under the Creative Commons Attribution 4.0 International (CC BY 4.0) license, which permits unrestricted use, distribution, and reproduction in any medium, provided that the original author and source are credited.

Figure 3. Standardized Precipitation Index (SPI) time series at the 1-, 3-, 6-, and 12-month timescales for the Afrânio meteorological station during the period from January 1950 to December 2012.



Source: Authors

The SPI-1 series exhibits pronounced short-term fluctuations and no evident long-term pattern. In contrast, the SPI-12 series displays a much smoother temporal evolution, despite the occurrence of extreme values ranging approximately from −3.5 to 3.0. This behavior is expected, as longer accumulation periods tend to attenuate short-term variability and emphasize persistent hydroclimatic conditions.

Table 2 summarizes the years in which extreme drought events (SPI ≤ −2) were recorded, as well as the corresponding peak intensity values identified for the SPI-1, SPI-3, SPI-6, and SPI-12 series.

Table 2. Years in which extreme drought events (SPI ≤ −2) were identified at each timescale, with the corresponding peak intensity (minimum SPI value) shown in parentheses

Time scale	Years of Occurrence (SPI ≤ −2)
SPI-1	No events
SPI-3	1956 (−2.40), 1959 (−2.92), 1963 (−2.36), 1970 (−3.39), 1976 (−3.81), 1981 (−2.13), 1993 (−3.45), 2003 (−2.12).
SPI-6	1956 (−2.23), 1963 (−2.34), 1970 (−2.18), 1976 (−4.00), 1993 (−3.25).
SPI-12	1976 (−3.47), 1993 (−2.10).

Source: Authors.

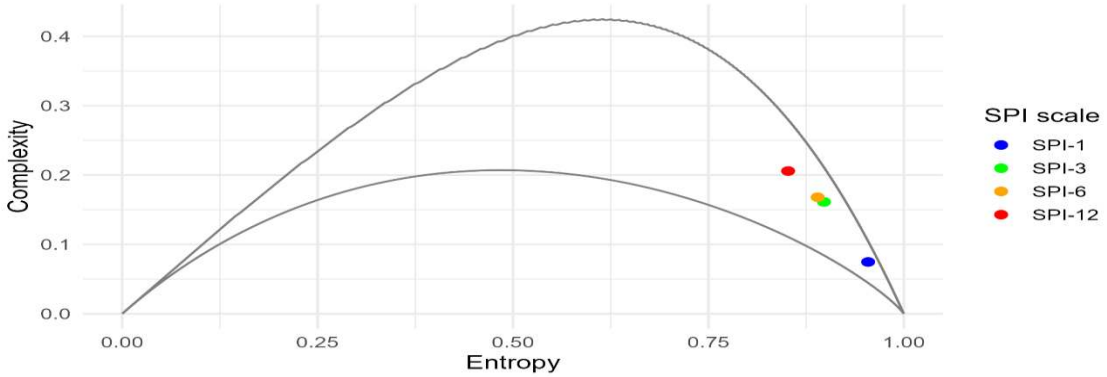
This article is published in open access under the Creative Commons Attribution 4.0 International (CC BY 4.0) license, which permits unrestricted use, distribution, and reproduction in any medium, provided that the original author and source are credited.

Table 2 shows that extreme drought events (SPI ≤ −2) were not detected at the 1-month timescale (SPI-1). Among the remaining timescales, the frequency of extreme droughts decreased as the accumulation period increased, with eight occurrences identified at SPI-3, five at SPI-6, and only two at SPI-12. The years 1976 and 1993 were the only ones in which drought conditions reached extreme intensity simultaneously across the 3-, 6-, and 12-month timescales.

The most severe drought event at all timescales occurred in 1976, with minimum SPI values of −3.81, −4.00, and −3.47 for SPI-3, SPI-6, and SPI-12, respectively. The second most intense event was recorded in 1993, reaching SPI values of −3.45, −3.25, and −2.10 at the same timescales. These results highlight the exceptional magnitude and persistence of the droughts that affected the region during these years.

To characterize the degree of randomness and the underlying temporal organization of the SPI series, the Complexity-Entropy Causality Plane (CECP) was employed. The resulting entropy-complexity representation is shown in Figure 4, where the continuous curves correspond to the theoretical upper and lower bounds of statistical complexity for the adopted embedding dimension (Rosso *et al.*, 2007, 2012). This framework enables the identification of distinct dynamical regimes and provides insights into the balance between stochasticity and temporal structure in the analyzed series.

Figure 4. Complexity-Entropy Causality Plane (CECP) for the SPI-1, SPI-3, SPI-6 and SPI-12 series derived from the Afrânio precipitation record from 01/1950 to 12/2012. The normalized permutation entropy (H_s) and statistical complexity (C) were calculated using an embedding dimension *d* = 5 and a time delay τ = 1.



Source: Authors.

This article is published in open access under the Creative Commons Attribution 4.0 International (CC BY 4.0) license, which permits unrestricted use, distribution, and reproduction in any medium, provided that the original author and source are credited.

Table 3. Permutation entropy (H_s) and statistical complexity (C) values obtained from the Complexity-Entropy Causality Plane (CECP) for the SPI series at the 1-, 3-, 6-, and 12-month timescales. Values computed for the full record (1950–2012) with embedding dimension *d* = 5 and time delay τ = 1.

SPI	Entropy (H_s)	Complexity (C)
SPI-1	0.954	0.075
SPI-3	0.898	0.161
SPI-6	0.890	0.168
SPI-12	0.852	0.206

Source: Authors.

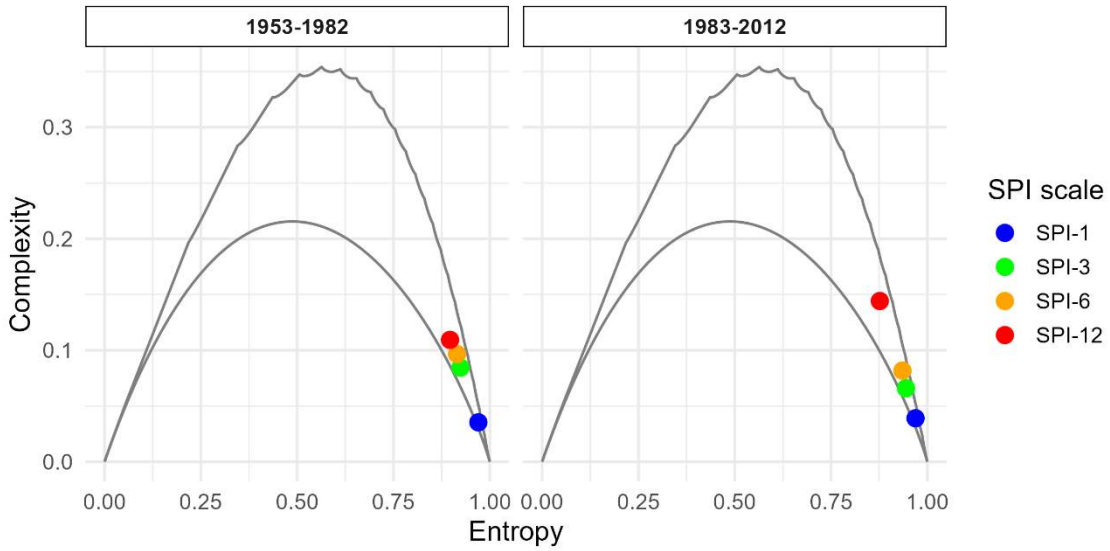
SPI-1 ($H_s = 0.954$, $C = 0.075$; Table 3) is located close to the white-noise region of the CECP, which reflects its high entropy and low statistical complexity. This position indicates a predominance of stochastic behavior and the absence of pronounced temporal organization or long-range correlations (Rosso *et al.*, 2007). As the accumulation timescale increases, entropy gradually decreases while statistical complexity increases (SPI-3: $H_s = 0.898$, $C = 0.161$; SPI-6: $H_s = 0.890$, $C = 0.168$; SPI-12: $H_s = 0.852$, $C = 0.206$). This systematic shift within the CECP suggests the emergence of greater temporal structure and persistence in medium-term (SPI-3 and SPI-6) and long-term (SPI-12) wet and dry conditions compared with the short-term variability represented by SPI-1.

The observed increase in complexity can be partly attributed to the influence of seasonal and interannual climatic variability, which becomes more evident as precipitation is accumulated over longer periods (Silva *et al.*, 2021b). However, the apparent gain in temporal organization associated with the smoothing of the series should be interpreted with caution. A portion of the increased temporal organization arises from the moving-sum procedure used in SPI computation, which inherently introduces deterministic autocorrelation into longer accumulation timescales (Lee *et al.*, 2026). Therefore, the shift toward lower entropy and higher complexity reflects both underlying hydroclimatic processes and methodological effects associated with the construction of the SPI.

To assess possible changes in the temporal dynamics of drought conditions over time, the historical series was partitioned into two 30-year subperiods (1953–1982 and 1983–2012). Figure 5 illustrates the location of the SPI series in the Complexity-Entropy Causality Plane (CECP) for each period, whereas Table 4 presents the corresponding values of the entropy and statistical complexity measures. Together, these results allow an evaluation of whether the dynamical properties of the SPI series have changed between the two climatological periods.

This article is published in open access under the Creative Commons Attribution 4.0 International (CC BY 4.0) license, which permits unrestricted use, distribution, and reproduction in any medium, provided that the original author and source are credited.

Figure 5. Complexity-Entropy Causality Plane (CECP) for the SPI-1, SPI-3, SPI-6 and SPI-12 series during the 1953–1982 and 1983–2012 subperiods. The normalized permutation entropy (H_s) and statistical complexity (C) were computed using an embedding dimension of *d* = 4 and a time delay τ = 1.



Source: Authors.

Table 4. Normalized permutation entropy (H_s) and statistical complexity (C) values obtained from the Complexity-Entropy Causality Plane (CECP) for the SPI series at the 1-, 3-, 6-, and 12-month timescales in the 1953–1982 and 1983–2012 subperiods. Values computed with embedding dimension *d* = 4 and time delay τ = 1; they should not be compared directly with those in Table 3.

SPI	1953–1982 (H_s)	1953–1982 (C)	1983–2012 (H_s)	1983–2012 (C)
SPI-1	0.970	0.035	0.969	0.039
SPI-3	0.924	0.084	0.945	0.066
SPI-6	0.915	0.097	0.935	0.082
SPI-12	0.897	0.109	0.877	0.144

Source: Authors

The comparison between the two 30-year subperiods revealed only subtle changes in the dynamical properties of the SPI series. At the 3- and 6-month timescales, the more recent period (1983–2012) exhibited higher entropy and lower statistical complexity than the earlier period

This article is published in open access under the Creative Commons Attribution 4.0 International (CC BY 4.0) license, which permits unrestricted use, distribution, and reproduction in any medium, provided that the original author and source are credited.

(1953–1982). This suggests more irregular medium-term wet and dry conditions, with weaker temporal organization. In contrast, at the annual timescale (SPI-12), entropy decreased while complexity increased in the second subperiod, which indicates a greater degree of temporal organization in long-term hydroclimatic conditions. These differences are small, and no significance test was applied. As in other studies that compare two periods with entropy-based measures (Silva *et al.*, 2022; Stosic *et al.*, 2026), the comparison is descriptive, and it should be read with caution.

These results indicate that the differences between the two periods were small and varied across timescales: the 3- and 6-month series showed slightly higher entropy in the second period, whereas the 12-month series showed slightly higher complexity. These patterns provide a starting point for further investigation of the climatic processes governing precipitation variability in the region.

The 1-month SPI (SPI-1) is primarily associated with meteorological drought and short-term impacts on soil moisture and crop development, particularly during the growing season. The 3-month SPI (SPI-3) reflects short- to medium-term moisture conditions, whereas the 6-month SPI (SPI-6) captures seasonal to medium-term variations in precipitation. In contrast, the 12-month SPI (SPI-12) is closely related to hydrological drought, as it reflects changes in streamflow, reservoir storage, and groundwater levels (Svoboda *et al.*, 2012).

Because the SPI is standardized relative to the long-term precipitation record for a given accumulation period, it provides a consistent measure of both water deficits and surpluses across multiple timescales. The position of SPI series within the Complexity-Entropy Causality Plane (CECP) makes it possible to characterize the degree of randomness, temporal organization, and complexity associated with wet and dry conditions at short-, medium-, and long-term timescales. Such information contributes to a better understanding of drought dynamics and may support decision-making in agricultural planning, drought monitoring, and water resources management in semi-arid regions.

4. CONCLUSION

In this study, the application of the Complexity-Entropy Causality Plane (CECP) to the Standardized Precipitation Index (SPI) helped describe how wet and dry conditions are organized over time in Afrânio, Pernambuco. The findings indicate that, at the monthly timescale (SPI-1), the local precipitation regime exhibits behavior closely resembling white noise, characterized by high entropy and low statistical complexity. This result shows weak memory in monthly rainfall. In

This article is published in open access under the Creative Commons Attribution 4.0 International (CC BY 4.0) license, which permits unrestricted use, distribution, and reproduction in any medium, provided that the original author and source are credited.

other words, short-term variability is mostly stochastic, although forecasting was not assessed in this work.

Regarding drought occurrence, extreme events (SPI ≤ −2) were identified at the 3-, 6-, and 12-month timescales, whereas no extreme droughts were detected in the SPI-1 series. Among all events, 1976 stands out as the most severe drought year at the 3-, 6- and 12-month timescales, followed by 1993. Notably, these were the only years in which drought conditions reached extreme intensity simultaneously at the 3-, 6-, and 12-month scales.

The CECP analysis of SPI-1, SPI-3, SPI-6, and SPI-12 showed a shift toward lower entropy and higher complexity from SPI-1 to SPI-12, with SPI-3 and SPI-6 very close to each other. Although this pattern suggests an apparent increase in temporal structure, it should not be interpreted as evidence of enhanced intrinsic hydrological predictability, which was not assessed in this study. Rather, it is partly attributable to the deterministic autocorrelation introduced by the moving-sum procedure inherent in SPI calculations over longer accumulation windows. Consequently, the observed increase in temporal organization reflects not only underlying hydroclimatic processes but also methodological effects associated with index construction.

A comparison of the two 30-year subperiods (1953–1982 and 1983–2012) showed small differences in entropy and complexity, with all SPI series remaining within the same dynamical region of the CECP. This descriptive comparison indicates that the main features of the SPI dynamics were broadly similar in the two periods, and it provides a baseline for future studies that include formal uncertainty assessment.

This study has limitations. It is based on a single station and a 63-year record. The differences between subperiods were not tested statistically. The SPI accumulation procedure adds autocorrelation to the series, which affects entropy and complexity at longer timescales. Finally, results may depend on the embedding dimension (d = 5 for the full series, d = 4 for the subperiods), so values from the two analyses should not be compared directly.

Using the CECP alongside SPI series helps describe how drought-related variability is organized across accumulation timescales in Afrânio. The same approach can be extended to other semi-arid stations to explore how drought dynamics vary across the region.

Acknowledgments: A.V.A.S. acknowledges the support of Coordenação de Aperfeiçoamento de Pessoal de Nível Superior - Brasil (CAPES) - Finance Code 001, Grant No. 88887.286895/2026-00. A.S.A.S. and T.S. acknowledge support of the Brazilian agency CNPq through the research grants 306590/2024-7 and 309499/2022-4.

This article is published in open access under the Creative Commons Attribution 4.0 International (CC BY 4.0) license, which permits unrestricted use, distribution, and reproduction in any medium, provided that the original author and source are credited.

REFERENCES

Bandt, C., & Pompe, B. (2002). Permutation entropy: A natural complexity measure for time series. *Physical Review Letters*, *88*(17), Article 174102. https://doi.org/10.1103/PhysRevLett.88.174102

Beltrão, B. A., Mascarenhas, J. C., Miranda, J. L. F., Souza Junior, L. C., Galvão, M. J. T. G., & Pereira, S. N. (2005). *Projeto cadastro de fontes de abastecimento por água subterrânea: Diagnóstico do município de Afrânio, estado de Pernambuco*. CPRM/PRODEEM.

Brito, S. S. B., Cunha, A. P. M. A., Cunningham, C. C., Alvalá, R. C., Marengo, J. A., & Carvalho, M. A. (2021). Monitoring meteorological drought in a semiarid region using two long-term satellite-estimated rainfall datasets: A case study of the Piranhas River basin, northeastern Brazil. *Atmospheric Research*, *250*, Article 105380. https://doi.org/10.1016/j.atmosres.2020.105380

Edwards, D. C., & McKee, T. B. (1997). *Characteristics of 20th century drought in the United States at multiple time scales* (Atmospheric Science Paper No. 634). Colorado State University.

Hayes, M., Svoboda, M., Wall, N., & Widhalm, M. (2011). The Lincoln Declaration on Drought Indices: Universal meteorological drought index recommended. *Bulletin of the American Meteorological Society*, *92*(4), 485–488. https://doi.org/10.1175/2010BAMS3103.1

Lamberti, P. W., Martin, M. T., Plastino, A., & Rosso, O. A. (2004). Intensive entropic non-triviality measure. *Physica A: Statistical Mechanics and its Applications*, *334*(1–2), 119–131. https://doi.org/10.1016/j.physa.2003.11.005

Lee, T., Kong, Y., Singh, V. P., & Yoon, H.-C. (2026). Autocorrelation structure of SPI and its implication for drought forecasting. *International Journal of Climatology*, *46*(4), Article e70240. https://doi.org/10.1002/joc.70240

McKee, T. B., Doesken, N. J., & Kleist, J. (1993). The relationship of drought frequency and duration to time scales. In *Proceedings of the Eighth Conference on Applied Climatology* (pp. 179–184). American Meteorological Society.

Palmer, W. C. (1965). *Meteorological drought* (Office of Climatology Research Paper No. 45). U.S. Weather Bureau.

Riedl, M., Müller, A., & Wessel, N. (2013). Practical considerations of permutation entropy. *The European Physical Journal Special Topics*, *222*(2), 249–262. https://doi.org/10.1140/epjst/e2013-01862-7

Rosso, O. A., Carpi, L. C., Saco, P. M., Gómez Ravetti, M., Plastino, A., & Larrondo, H. A. (2012). Causality and the entropy-complexity plane: Robustness and missing ordinal patterns. *Physica A: Statistical Mechanics and its Applications*, *391*(1), 42–55. https://doi.org/10.1016/j.physa.2011.07.030

Rosso, O. A., Larrondo, H. A., Martin, M. T., Plastino, A., & Fuentes, M. A. (2007). Distinguishing noise from chaos. *Physical Review Letters*, *99*(15), Article 154102. https://doi.org/10.1103/PhysRevLett.99.154102

This article is published in open access under the Creative Commons Attribution 4.0 International (CC BY 4.0) license, which permits unrestricted use, distribution, and reproduction in any medium, provided that the original author and source are credited.

Santiago, E. J. P., Silva, L. P., Gomes-Silva, F., & Silva, A. S. A. (2019). Precipitação provável para o município de Afrânio-PE em diferentes níveis probabilístico. *Sigmae*, *8*(2), 437–448. https://publicacoes.unifal-mg.edu.br/revistas/index.php/sigmae/pt_BR/article/view/1026

Silva, A. S. A., Barreto, I. D. d. C., Cunha-Filho, M., Menezes, R. S. C., Stosic, B., & Stosic, T. (2022). Spatial and temporal variability of precipitation complexity in Northeast Brazil. *Sustainability*, *14*(20), Article 13467. https://doi.org/10.3390/su142013467

Silva, A. S. A., Menezes, R. S. C., Rosso, O. A., Stosic, B., & Stosic, T. (2021a). Complexity-entropy analysis of monthly rainfall time series in northeastern Brazil. *Chaos, Solitons & Fractals*, *143*, Article 110623. https://doi.org/10.1016/j.chaos.2020.110623

Silva, A. S. A., Menezes, R. S. C., Telesca, L., Stosic, B., & Stosic, T. (2021b). Fisher–Shannon analysis of drought/wetness episodes along a rainfall gradient in Northeast Brazil. *International Journal of Climatology*, *41*(S1), e2751–e2765. https://doi.org/10.1002/joc.6834

Silva, M. D. P. B. da, Oliveira, V. P. V. de, Silva, M. L. da, Silveira, V. L. da, Oliveira, J. P. de, Oliveira, M. de A., & Assunção Filho, F. A. F. (2025). Drought in northeast Brazil: History, climatic and social implications. *Revista Brasileira de Climatologia*, *37*(21), 820–842. https://doi.org/10.55761/abclima.v37i21.19848

Stosic, T., Tošić, I., Silva, A. S. A., Djurdjević, V., & Stosic, B. (2026). Spatiotemporal variation in rainfall predictability in Serbia under a changing climate. *Nonlinear Processes in Geophysics*, *33*(1), 157–172. https://doi.org/10.5194/npg-33-157-2026

Svoboda, M., Hayes, M., & Wood, D. A. (2012). *Standardized precipitation index user guide* (WMO-No. 1090). World Meteorological Organization.

Thom, H. C. S. (1966). *Some methods of climatological analysis* (WMO Technical Note No. 81). Secretariat of the World Meteorological Organization.

Vicente-Serrano, S. M., Beguería, S., & López-Moreno, J. I. (2010). A multiscalar drought index sensitive to global warming: The standardized precipitation evapotranspiration index. *Journal of Climate*, *23*(7), 1696–1718. https://doi.org/10.1175/2009JCLI2909.1

Vieira, A. F. F., & Lira, D. R. de. (2025). Influência dos eventos de teleconexão El Niño-Oscilação Sul e Dipolo do Atlântico Tropical na ocorrência de anos secos em um município do São Francisco pernambucano. In *Anais do XVI Simpósio Brasileiro de Climatologia Geográfica* (pp. 1836–1850). https://static.even3.com/anais/1137921.pdf

Wilks, D. S. (2011). *Statistical methods in the atmospheric sciences* (3rd ed.). Academic Press.

This article is published in open access under the Creative Commons Attribution 4.0 International (CC BY 4.0) license, which permits unrestricted use, distribution, and reproduction in any medium, provided that the original author and source are credited.